Coaxial Nanocables of AlN Nanowire Core and Carbon/BN Nanotube Shell

ARTICLE *in* THE JOURNAL OF PHYSICAL CHEMISTRY C · DECEMBER 2007

Impact Factor: 4.77 · DOI: 10.1021/jp076217y

2 AUTHORS, INCLUDING:

Zhen Zhou
Nankai University
213 PUBLICATIONS **6,993** CITATIONS

SEE PROFILE

Coaxial Nanocables of AlN Nanowire Core and Carbon/BN Nanotube Shell

Zhen Zhou*,† and Shigeru Nagase‡

Institute of New Energy Material Chemistry, Institute of Scientific Computing, Nankai University, Tianjin 300071, People's Republic of China, and Department of Theoretical Molecular Science, Institute for Molecular Science, Myodaiji, Okazaki 444-8585, Japan

Received: August 3, 2007; In Final Form: October 1, 2007

Using density functional theory (DFT), we investigated the nanocable models comprised of AlN crystalline nanowires as cores and single-walled carbon nanotubes (SWCNTs) or BN nanotubes (BNNTs) as shells. The AlN@SWCNT nanocable is assembled by a weak van der Waals interaction. The optimum tube−wire distance is ∼0.35 nm with an insertion energy of 0.07 eV per AlN. Accordingly, the band structures are superpositions of those of their separate components. The insertion of the AlN nanowire inside BNNTs is more favorable than that inside SWCNTs with comparable diameters. The most favorable case for AlN@BNNT shows that the tube−wire distance is ∼0.30 nm and that the insertion energy is 0.09 eV per AlN. The insertion narrows the band gap of AlN nanowires by ∼0.21 eV. Exothermic insertion can also be realized at the tube−wire distance of ∼0.22 nm by the formation of strong bonding between AlN nanowires and BNNTs, and this nanocable is changed into a *p*-type semiconductor. The interaction revealed in the present nanocable models is helpful for understanding other inorganic compound nanowire−nanotube hybrid systems.

Introduction

Stimulated by carbon nanotubes (CNTs),[1] a number of inorganic nanowires/tubes have been prepared with diameters of a few nanometers and lengths up to several micrometers, and their active chemical reactivity due to a high surface-to-volume ratio and changes in physical properties by dimensionality and size confinement have been extensively investigated to explore their potential applications in catalysis, gas sensors, medical diagnostics, lasers, field-emission transistors, etc.[2] Inorganic nanowires/tubes provide one-dimensional (1-D) transport in nanoscale electronics and optoelectronics, but they will be disturbed by unwanted interactions with neighboring nanowires and foreign molecules. Therefore, another variety of 1-D nanomaterials, nanocables, is proposed. Initially the nanocables found experimentally referred to the coaxial structures of several layers of nanotubes and/or clusters. In 1997, Colliex et al. found a sandwich C−BN−C structure closely resembling a coaxial nanocable.[3] In 1998, Zhang et al. reported coaxial nanocable structures consisting of a β-phase silicon carbide core, an amorphous silicon oxide intermediate layer, and separated C/BN layered radial outer shells.[4] Coaxial nanocables have already been demonstrated as gated field-effect transistors and quantum wire lasers.[5] In this work, we investigated coaxial nanocables composed of nanowires and nanotubes.

Many coaxial nanocables composed of nanowires and carbon/BN nanotubes have been prepared experimentally. CNTs can be filled with metal and inorganic compound nanowires by capillarity or wet-chemistry methods that have been performed successfully for a decade.[6] Very recently, it has been found that a sample of Damascus sabre steel from the 17th century even contained CNTs filled with cementite nanowires.[7] Novel electronic and magnetic properties of metal-filled CNTs have been predicted.[8] BN nanotubes (BNNTs) are ideal insulating sheaths for encapsulating chemically active nanowires.[9] Because of the ionic bonding character, BNNTs possess many properties different from those of CNTs.[10] In particular, BNNTs have stable insulating properties (∼5.5 eV band gap) weakly dependent on the diameter, helicity, and tubewall number.[11] Moreover, BNNTs are chemically inert and thermally stable.[12] In many reports, BNNTs were successfully filled with Ni, Co, Fe, or Cu metal wires, Fe−Ni, $NiSi_2$ alloys,[13] oxides such as α-Al_2O_3[14] and $Al_{18}B_4O_{33}$,[15] SiC carbides,[16,17] Si_3N_4[17] and GaN nitrides,[18,19] and potassium halide nanowires.[20] The unique use of BNNTs leads to novel functional materials (e.g., the surface addition of BN greatly enhances the electron field-emission characteristics of CNTs, Si tips, and GaN films).[21]

Computational simulation and theoretical investigation are necessary to understand unique nanoscale phenomena. Single-walled carbon nanotubes (SWCNTs) filled with metal wires have been studied through density functional theory (DFT) computations. It was found that there is a strong coupling between encapsulated transition metal (Fe, Co, etc.) wires and SWCNTs, which leads to substantial modification of their electronic structures.[8] DFT studies have also been performed for BNNTs filled with transition metal wires such as Ni,[22,23] Co,[23] and Cu.[24] Unlike the case of SWCNTs, all these nanocables are assembled by weak van der Waals (vdW) interactions, and the electronic structures of the metal wires are not disturbed by the outer BN sheath. Cu@BNNT hybrid materials are ideal nanocables with a conducting core and insulating sheath,[24] and BNNTs filled with Co, Ni, etc. show a high spin polarization at the Fermi level, which leads to potential spintronic applications.[23]

However, there is no DFT study on nanocables composed of inorganic compound nanowires and BN/C nanotubes, partly due to the difficulty in finding proper computational models where nanowires have matching lattices in the axial direction to SWCNTs or BNNTs. Such matching is critical for the periodic

* Corresponding author. E-mail: zhouzhen@nankai.edu.cn.
† Nankai University.
‡ Institute for Molecular Science.

10.1021/jp076217y CCC: $37.00
Published on Web 11/21/2007

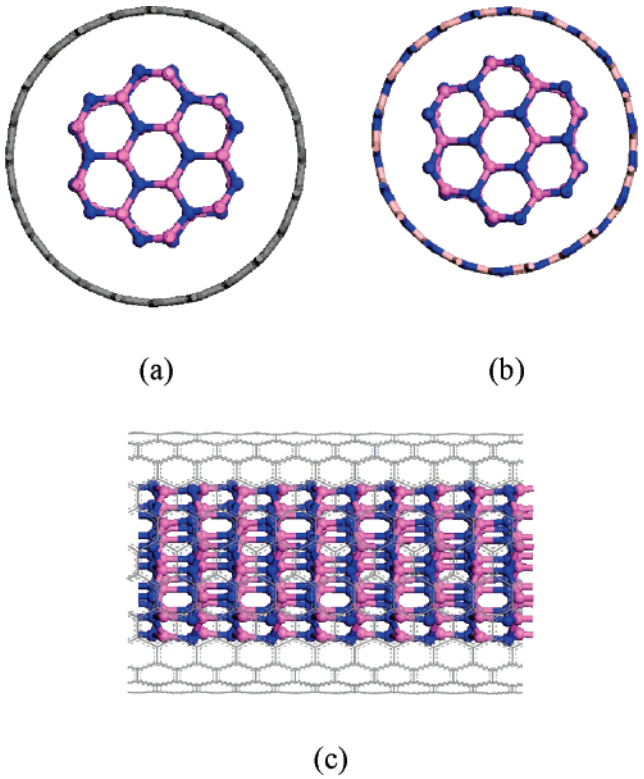

Figure 1. Structures of AlN nanowires filled inside (12,12) SWCNT (a) and (11,11) BNNT (b). Panel c is the side view of panel a with five repeated unit cells.

boundary condition (PBC) computations. Since the lattice parameter, *c*, of the AlN nanowire unit cell (4.95 Å) basically matches the lattice parameter of the unit cells of armchair SWCNTs and BNNTs (~4.9 Å), they were chosen as prototypes to represent a variety of nanocables composed of inorganic compound nanowires and BN/C nanotubes. AlN is an important wide band gap semiconductor with many applications in electronic elements and light emitting devices. AlN nanowires/tubes are usually synthesized with a single-crystalline wurtzite structure along the [0001] growth direction. Using the AlN−BN/C nanocable models, we attempted to clarify the interaction between inorganic compound nanowires and BN/C nanotube sheaths and the changes in their electronic structures.

Computational Methods

As shown in Figure 1, AlN crystalline nanowires in SWCNTs or BNNTs are coaxially placed in a periodically repeating tetragonal supercell with a dimension of 30 Å × 30 Å × *c* Å (*c* is the length in the axial direction of the AlN nanowire unit cell and comparable to twice the corresponding length of the armchair BN/C nanotube unit cell), so that infinitely long (rather than truncated) 1-D systems are simulated and the interaction between nearest-neighbor wires or tubes is negligible. (*n*,*n*) SWCNTs ($n = 10-13$) and BNNTs ($n = 9-12$) were considered for the encapsulation of AlN nanowires. Starting from the initial models, the coordinates of all the atoms within the supercell were fully relaxed, and the lattice constant, *c*, was also optimized to minimize the total energy and stress along the tube/wire axis.

DFT computations were performed using a plane-wave pseudo-potential technique implemented in the Vienna ab initio simulation package (VASP).[25,26] The local density approximation (LDA) with the CA functional[27] and a 360 eV cutoff for the plane-wave basis set were used for all geometry optimizations. The core electrons were modeled by the ultrasoft pseudopotential.[28] Five *k* points were used for sampling the 1-D Brillouin zone along the tube/wire axis, and the convergence thresholds were set to be 10^{-4} eV in energy and 10^{-3} eV/Å in force. On the basis of equilibrium structures, 21 *k* points were then used to obtain band structures.

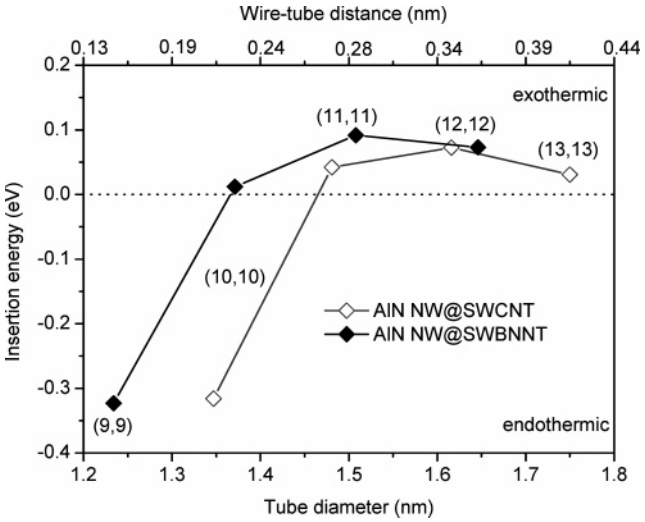

Figure 2. Insertion energies per AlN for the AlN nanowire filled inside various SWCNTs and BNNTs as a function of tube diameter.

Results and Discussion

The AlN crystalline nanowire was coaxially placed inside a series of armchair nanotubes, from (9,9) to (12,12) for BNNTs with tube diameters between 1.23 and 1.65 nm and from (10,10) to (13,13) for SWCNTs with tube diameters between 1.35 and 1.75 nm. The cable structures were fully optimized, and the calculated insertion energies are shown in Figure 2. The insertion energy is defined as $E_i = E_{tot}(\text{tube}) + E_{tot}(\text{wire}) - E_{tot}(\text{tube + wire})$.

Figure 2 shows that the insertion of the AlN wire into SWCNTs and BNNTs with smaller diameters is considerably endothermic. As the tube diameter increases, the insertion becomes exothermic. The largest insertion energy is ~0.09 eV per AlN for AlN@(11,11) BNNT with a 1.51 nm diameter, while it is ~0.07 eV for AlN@(12,12) SWCNT with a 1.62 nm diameter. The insertion energies become smaller when the tube diameters further increase because of larger tube−wire distances. Therefore, the (11,11) BNNT and (12,12) SWCNT are the best outer sheaths to encapsulate the AlN nanowire, as shown in Figure 1. Since the AlN nanowires with faceted surfaces are not round, we can only estimate the shortest distance between the AlN nanowire and the BN/C nanotubes. The shortest wire−tube distances are 0.30 and 0.35 nm for the most stable AlN@BNNT and AlN@SWCNT, respectively. As is apparent from Figure 2, larger SWCNTs are needed for encapsulating a given AlN nanowire, as compared to BNNTs. In addition, the insertion of the AlN nanowire inside SWCNTs is all less favorable than that inside BNNTs with comparable diameters. For the most stable structures, the insertion energy of the AlN@(11,11) BNNT is 0.02 eV larger than that of the AlN@(12,12) SWCNT. Another interesting difference is that even the insertion of the AlN nanowire inside (10,10) BNNT with a smaller diameter of ~1.37 nm is already exothermic (0.01 eV per AlN), and the tube−wire distance is only 0.22 nm. In contrast, the insertion of the AlN nanowire inside the (10,10) SWCNT, which leads to a smaller wire−tube distance of 0.28

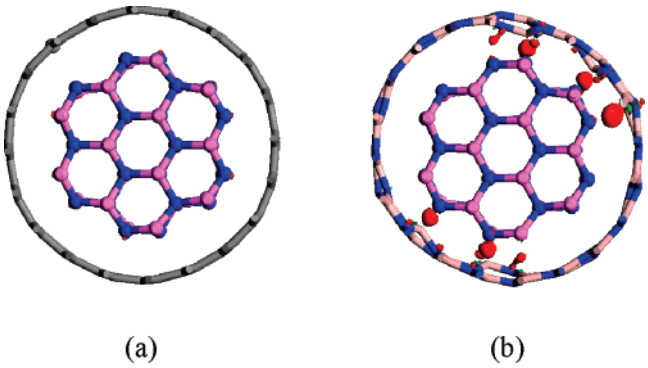

Figure 3. Isosurface for the electronic density difference after the AlN nanowire is inserted inside (10,10) SWCNT (a) and BNNT (b). Red means an increase in electronic density, while green means a decrease in electronic density. Electronic density increases apparently between AlN nanowire and BNNT. AlN@(10,10) BNNT and AlN@(10,10) SWCNT have the same amount of valence electrons, so the electronic density difference can be compared within the same isosurface value.

TABLE 1: E_i, DEF, and INT per AlN for Various Nanocables

	E_i (eV)	DEF (eV)	INT (eV)
AlN@(10,10) BNNT	0.01	−0.48	0.49
AlN@(11,11) BNNT	0.09	−0.04	0.14
AlN@(10,10) SWCNT	−0.32	−0.20	−0.12
AlN@(11,11) SWCNT	0.04	−0.02	0.06
AlN@(12,12) SWCNT	0.07	−0.01	0.08

nm, is endothermic by 0.32 eV. This suggests that there is a strong interaction between the AlN nanowire and the BNNTs.

The optimized structures and isosurfaces for the electronic density difference of AlN@(10,10) SWCNT and AlN@(10,-10) BNNT are shown in Figure 3. In Figure 3, the electronic density increases apparently between AlN and BNNT after the insertion of the AlN nanowire, but there is no apparent change in the cable of the AlN@(10,10) SWCNT within the same isosurface value. There is a strong interaction between AlN and BNNT, which leads to the dramatic deformation of the (10,10) BNNT. The distances between B atoms in the BNNT and N atoms in the AlN wire are in the range of 1.59−1.61 Å, approaching the B−N bond length in the sp^3-hybridized cubic BN phase (1.567 Å).[29] Also, weaker bonding appears between the N atoms in BNNT and the Al atoms in the AlN nanowire surface, with distances of 2.22−2.28 Å.

Because of the hexagonal morphology of the AlN nanowire, wires and tubes are geometrically deformed so as to obtain a maximum attractive interaction. In this case, the insertion energy (E_i) in Figure 2 can be expressed as the sum of the intramolecular deformation (DEF) energy and the intermolecular interaction (INT) energy. In the exothermic insertion, the destabilization due to DEF is overcome by the stabilization due to INT. The previous corresponding energies are summarized in Table 1 for various nanocables. The INT energy of the AlN@-(10,10) BNNT is as large as 0.49 eV per AlN, so there is strong bonding between AlN wires and BNNTs. On the contrary, the INT energy of the AlN@(10,10) SWCNT is −0.12 eV per AlN, indicating that there is a strong repulsive interaction between the AlN nanowire and the (10,10) SWCNT. Such repulsive interaction and structural deformation make the insertion of the AlN nanowire into the (10,10) SWCNT highly endothermic, and the nanocable is rather unstable. In the most stable nanocable AlN@BN (11,11), the outer BNNT sheath also shows some deformation after the insertion of the AlN nanowire. As for AlN@SWCNT (12,12), only slight changes in the geometries occur in going to the nanocable. The INT energies are 0.14 and 0.08 eV for AlN@(11,11) BNNT and AlN@(12,12) SWCNT, respectively. It is easy to understand that the B−N bonds in BNNTs and Al−N bonds in AlN nanowires are all partly ionic; moreover, there are dangling bonds in the lateral surfaces of AlN nanowires, so attractive interaction is much easier to occur between AlN nanowires and BNNTs. However, the bonding in SWCNTs is conjugated π characteristic and nonpolar, so it is difficult for attractive interactions to occur.

The interaction between outer nanotubes and inner AlN wires was also investigated by computing the band structures for the AlN@(12,12) SWCNT (Figure 1a) and the AlN@(11,11) BNNT (Figure 1b) nanocables, and the results are shown in Figures 4 and 5, as compared to those of their separate components. In Figure 4, the AlN nanowire shows a wide band gap of ∼3.30 eV, which is much smaller than that of bulk AlN (the calculated DFT result is ∼4.22 eV[30]) because some surface states associated with the three-fold coordinated N and Al atoms at lateral facets in nanowires appear at both valence and conduction band edges.[31] The (12,12) SWCNT is typically metallic with two bands crossing the Fermi level. Because of the weak interaction, the band structure for the AlN@(12,12) SWCNT nanocable is clearly a superposition of those of the individual (12,12) SWCNT and AlN wires. Although the nanocable is also metallic, the bands crossing the Fermi level all originate from the outer SWCNT sheath, whereas the inner AlN wire remains a semiconductor with a wide band gap.

In Figure 5, the (11,11) BNNT shows a wide band gap of ∼4.69 eV and can be regarded as an insulator. The insertion of the AlN nanowire inside BNNTs does not change the band structure apparently, and the conduction band maximum (CBM) and the valence band minimum (VBM) both originate basically from the AlN nanowire. However, after carefully checking the band structure, we find that the band gap of the nanocable is only ∼3.09 eV, 0.21 eV smaller than that of the isolated AlN nanowire. It is known that the lateral surface of AlN and other inorganic compound nanowires is very susceptible to adsorbed molecules or functional groups. For example, the hydrogen termination[31] and NH_3 adsorption[30] were found to narrow the band gap. An obvious red-shift was experimentally found for the photoluminescence spectrum of GaN nanowires coated with BN,[9] which may also be attributable to the interaction between the outer BN sheath and the inner nanowires. Figure 6 shows the isosurface for the electron density of the top valence band and bottom conduction band of the AlN@(11,11) BNNT. It is apparent that there is still a considerably strong interaction between the inner AlN wire and the outer BNNTs. Such an interaction disturbs both the valence and the conduction band edges, especially the conduction band bottom. Therefore, the band gap of the nanocable is narrowed.

The band structure for the nanocable in Figure 3b is shown in Figure 5c. It is interesting that the strong interaction between the outer BNNT and the inner AlN nanowire changes the nanocable into a *p*-type semiconductor. The interaction in the AlN@(10,10) BNNT can clearly be seen from the density of states (DOS) in Figure 7. The B and N atoms in BNNTs show great hybridization correspondingly with the N and Al atoms in the lateral surface of the AlN nanowire. In the new cable, the valence band edge consists mainly of N atoms in the lateral surface of the AlN nanowire, but the B atoms in BNNT almost contribute to the conduction band, indicating that there is a strong interaction between the B atoms in BNNT and the N atoms in the wire lateral surface with dangling bonds. Such an interaction makes the nanocable a new semiconductor with a

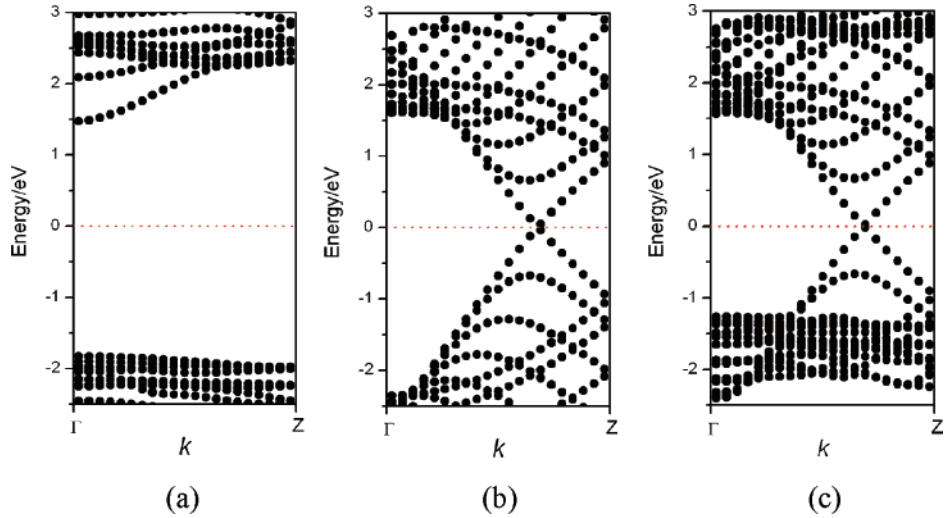

Figure 4. Band structures for the AlN nanowire (a), (12,12) SWCNT (b), and nanocable of AlN@(12,12) SWCNT (c). Dotted lines denote the position of the Fermi level.

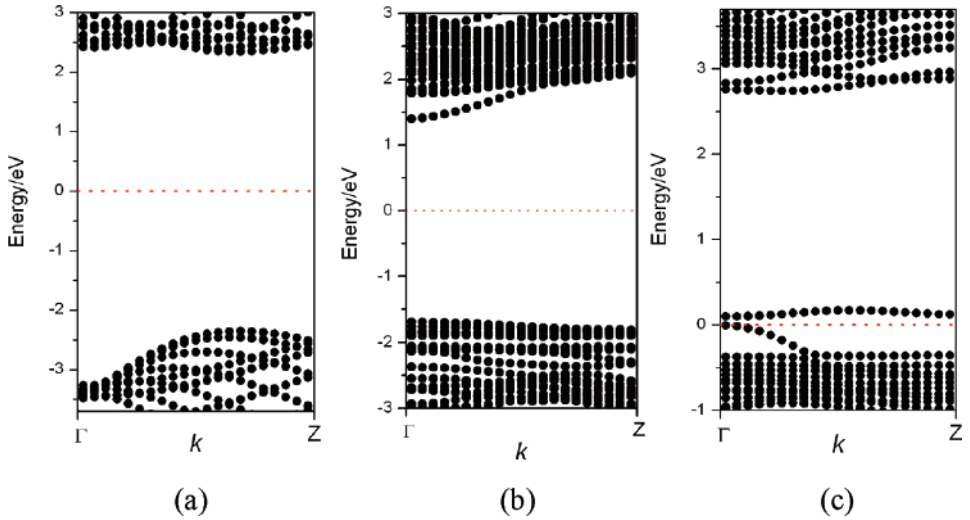

Figure 5. Band structures of (11,11) BNNT (a) and nanocables of AlN@(11,11) BNNT (b) and AlN@(10,10) BNNT (c). Dotted lines denote the position of the Fermi level.

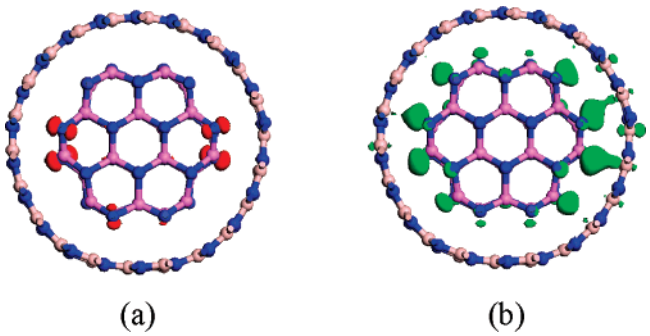

Figure 6. Isosurface for the electron density of the top valence band (a) and the bottom conduction band (b) of AlN@(11,11) BNNT. The top valence band mainly originates from the inner AlN nanowire, especially in the region close to the outer BNNT, and it is more apparent that the region of the tube and wire with strong interaction contributes to the conduction band bottom.

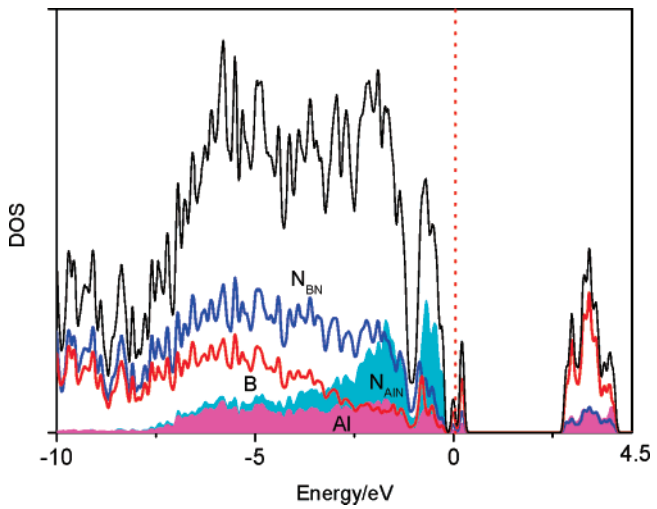

Figure 7. Total density of states (TDOS) for the nanocable of AlN@BN (10,10) BNNT and projected density of states (PDOS) for the Al and N atoms in the lateral surface of the AlN nanowire and B and N atoms in BNNT. Dotted line denotes the position of the Fermi level.

narrower band gap of ~2.70 eV. Also, acceptor levels appear above the VBM, so the newly formed semiconductor is a *p*-type.

From the previous results, we have clarified the electronic properties and the nature of the tube−wire interaction in the nanocables of AlN@BN/C nanotubes. These models are not only illustrative but are useful for other systems involving nitride and probably oxide nanowires to fill inside SWCNTs or BNNTs. Since nitrides and oxides have polar bonding, they are expected

to interact strongly with BNNTs. Accordingly, some new hybrid core−shell structures may be attained with unexpected electronic structures that are useful in technology. Large BNNTs can encapsulate AlN nanowires with weak interactions (Figure 1b); however, in practical material systems, the encapsulated wires would grow adjacently to inner walls of the BNNTs and not form a coaxial structure. CNTs with nonpolar chemical bonding have a weak interaction with the encapsulated inorganic compound nanowires, so the hybrid nanocables are assembled under vdW interactions, and the electronic characteristic of the inorganic compound nanowires will not be disturbed. Therefore, CNTs can be used as templates to synthesize ultrathin inorganic compound nanowires.

Conclusion

In summary, we performed a comparative DFT investigation on nanocables composed of AlN crystalline nanowire and SWCNTs or BNNTs. The interaction in the AlN@BNNT nanocables is different from that in the AlN@SWCNTs. The insertion of the AlN nanowire into SWCNTs is less favorable than that into BNNTs with comparable diameters. The optimum tube−wire distance is ∼0.30 nm with an insertion energy of 0.09 eV for BNNTs and ∼0.35 nm with an insertion energy of 0.07 eV for SWCNTs. A tube−wire distance of only 0.22 nm can realize the exothermic insertion of the AlN nanowire into BNNTs because of strong bonding between AlN nanowire and BNNTs. These results are in sharp contrast to the insertion of metal wires inside SWCNTs[8] and BNNTs[22−24] because metal wires have strong bonding with SWCNTs, while they are assembled inside BNNTs under weak vdW interactions.

The electronic band structures of the AlN@SWCNT nanocables are superpositions of those from the isolated individual components. AlN@BNNT nanocables show some changes in band structures; the encapsulation makes the band gap of the AlN nanowire narrower by ∼0.21 eV in the most stable nanocable, and the nanocable of the AlN nanowire filled inside a smaller BNNT is a *p*-type semiconductor.

Cable-like nanomaterials have potential applications in nanotechnology. The assembling mechanism clarified in the present study is applicable to the insertion of other inorganic compound nanowires inside SWCNTs or BNNTs.

Acknowledgment. This study was supported by NSFC (50502021) and NKStar HPC Program in China and by a Grant-in-Aid for Scientific Research on Priority Area and the Next Generation Supercomputing Project (Nanoscience Program) from the MEXT of Japan.

References and Notes

(1) Iijima, S. *Nature (London, U.K.)* **1991**, *354*, 56.

(2) See recent reviews and references therein: (a) Goldberger, J.; Fan, R.; Yang, P. D. *Acc. Chem. Res.* **2006**, *39*, 239. (b) Remskar, M. *Adv. Mater.* **2004**, *16*, 1497. (c) Rao, C. N. R.; Nath, M. *Dalton Trans.* **2003**, *1*, 1. (d) Rao, C. N. R.; Govindaraj, A.; Vivekchand, S. R. C. *Annu. Rep. Prog. Chem. A* **2006**, *102*, 20. (e) Tenne, R.; Rao, C. N. *R. Phil. Trans. R. Soc. London, Ser. A* **2004**, *362*, 2099. (f) Rao, C. N. R.; Deepak, F. L.; Gundiah, G.; Govindaraj, A. *Prog. Solid State Chem.* **2003**, *31*, 5.

(3) Suenaga, K.; Colliex, C.; Demoncy, N.; Loiseau, A.; Pascard, H.; Willaime, F. *Science (Washington, DC, U.S.)* **1997**, *278*, 653.

(4) Zhang, Y.; Suenaga, K.; Colliex, C.; Iijima, S. *Science (Washington, DC, U.S.)* **1998**, *281*, 973.

(5) (a) Lauhon, L. J.; Gudiksen, M. S.; Wang, D. L.; Lieber, C. M. *Nature (London, U.K.)* **2002**, *420*, 57. (b) Choi, H.-J.; Johnson, J. C.; He, R.; Lee, S.-K.; Kim, F.; Pauzauskie, P.; Goldberger, J.; Saykally, R. J.; Yang, P. *J. Phys. Chem. B* **2003**, *107*, 8721.

(6) (a) Zhao, J. J.; Xie, R. H. J. *Nanosci. Nanotechnol.* **2003**, *3*, 459 and references therein. (b) Zhang, Y.; Han, W.; Gu, G. Nanocables and Nanojunctions. In *Encyclopedia of Nanoscience and Nanotechnology*; Nalwa, H. S., Ed.; American Scientific Publishers: Stevenson Ranch, CA, 2004; Vol. 6, pp 61−76.

(7) Reibold, M.; Paufler, P.; Levin, A. A.; Kochmann, W.; Pätzke, N.; Meyer, D. C. *Nature (London, U.K.)* **2006**, *444*, 286.

(8) (a) Yang, C. K.; Zhao, J.; Lu, J. P. *Phys. Rev. Lett.* **2003**, *90*, 257203. (b) Yang, C. K.; Zhao, J.; Lu, J. P. *Int. J. Nanosci.* **2004**, *4*, 561. (c) Gao, X. P.; Zhang, Y.; Chen, X.; Pan, G. L.; Yan, J.; Wu, F.; Yuan, H. T.; Song, D. Y. *Carbon* **2004**, *42*, 47. (d) Kang, Y. J.; Choi, J.; Moon, C. Y.; Chang, K. J. *Phys. Rev. B: Condens. Matter Mater. Phys.* **2005**, *71*, 115441. (e) Fujima, N.; Oda, T. *Phys. Rev. B: Condens. Matter Mater. Phys.* **2005**, *71*, 115412. (f) Yang, C. K.; Zhao, J. J.; Lu, J. P. *Phys. Rev. B: Condens. Matter Mater. Phys.* **2002**, *66*, 41403. (g) Ivanovskaya, V. V.; Köhler, C.; Seifert, G. *Phys. Rev. B: Condens. Matter Mater. Phys.* **2007**, *75*, 75410.

(9) (a) Gleize, P.; Schouler, M. C.; Gadelle, P.; Caillet, M. *J. Mater. Sci.* **1994**, *29*, 1575. (b) Chopra, N. G.; Luyken, R. J.; Cherrey, K.; Crespi, V. H.; Cohen, M. L.; Louie, S. G.; Zettl, A. *Science (Washington, DC, U.S.)* **1995**, *269*, 966. (c) Ma, R. Z.; Bando, Y.; Sato, T.; Kurashima, K. *Chem. Mater.* **2001**, *13*, 2965. (d) Ma, R. Z.; Golberg, D.; Bando, Y.; Sasaki, T. *Philos. Trans. R. Soc. London, Ser. A* **2004**, *362*, 2161.

(10) (a) Golberg, D.; Bando, Y.; Tang, C. C.; Zhi, C. Y. *Adv. Mater.* **2007**, *19*, 2413. (b) Zhou, Z.; Zhao, J. J.; Gao, X. P.; Chen, Z. F.; Yan, J.; Schleyer, P. v. R.; Morinaga, M. *Chem. Mater.* **2005**, *17*, 992. (c) Zhou, Z.; Zhao, J. J.; Chen, Z. F.; Gao, X. P.; Yan, T. Y.; Schleyer, P. v. R. *J. Phys. Chem. B* **2006**, *110*, 13363. (d) Chen, X.; Gao, X. P.; Zhang, H.; Zhou, Z.; Hu, W. K.; Pan, G. L.; Zhu, H. Y.; Yan, T. Y.; Song, D. Y. *J. Phys. Chem. B* **2005**, *109*, 11525. (e) Zhou, Z.; Zhao, J. J.; Chen, Z. F.; Schleyer, P. v. R. *J. Phys. Chem. B* **2006**, *110*, 25678.

(11) Rubio, A.; Corkill, J. L.; Cohen, M. L. *Phys. Rev. B: Condens. Matter Mater. Phys.* **1994**, *49*, 5081.

(12) Chen, Y.; Zou, J.; Campbell, S. J.; Caer, G. L. *Appl. Phys. Lett.* **2004**, *84*, 2430.

(13) (a) Golberg, D.; Xu, F. F.; Bando, Y. *Appl. Phys. A* **2003**, *76*, 479. (b) Ma, R. Z.; Bando, Y.; Sato, T. *Chem. Phys. Lett.* **2004**, *350*, 1. (c) Golberg, D.; Bando, Y.; Kurashima, K.; Sato, T. *J. Nanosci. Nanotechnol.* **2001**, *1*, 49. (d) Tang, C. C.; Bando, Y.; Golberg, D.; Ding, X. X.; Qi, S. R. *J. Phys. Chem. B* **2003**, *107*, 6539. (e) Shelimov, K. B.; Moskovits, M. *Chem. Mater.* **2000**, *12*, 250.

(14) Ma, R. Z.; Bando, Y.; Sato, T. *Adv. Mater.* **2002**, *14*, 366.

(15) Song, H. S.; Zhang, J.; Lin, J.; Liu, S. J.; Lou, J. J.; Huang, Y.; Elssfah, E. M.; Elsanousi, A.; Ding, X. X.; Gao, J. M.; Tang, C. *J. Phys. Chem. C* **2007**, *111*, 1136.

(16) Li, Y. B.; Dorozhkin, P. S.; Bando, Y.; Golberg, D. *Adv. Mater.* **2005**, *17*, 545.

(17) Tang, C. C.; Bando, Y.; Sato, T.; Kurashima, K. *J. Mater. Chem.* **2002**, *12*, 1910.

(18) Han, W. Q.; Zettl, A. *Appl. Phys. Lett.* **2002**, *81*, 5051.

(19) Zhang, J.; Zhang, L. D.; Jiang, F. H.; Dai, Z. H. *Chem. Phys. Lett.* **2004**, *383*, 423.

(20) Han, W. Q.; Chang, C. W.; Zettl, A. *Nano Lett.* **2004**, *4*, 1355.

(21) (a) Park, N.; Ihm, J. *Bull. Am. Phys. Soc.* **2002**, *47*, 1013. (b) Kimura, C.; Yamamoto, T.; Hori, T.; Sugino, T. *Appl. Phys. Lett.* **2001**, *79*, 4533. (c) Sugino, T.; Kawasaki, S.; Tanioka, K.; Shirafuji, J. *Appl. Phys. Lett.* **1997**, *71*, 2704.

(22) Xiang, H. J.; Yang, J. L.; Hou, J. G.; Zhu, Q. S. *New J. Phys.* **2005**, *7*, 39.

(23) Yang, C. K.; Zhao, J. J.; Lu, J. P. *Phys. Rev. B: Condens. Matter Mater. Phys.* **2006**, *74*, 235445.

(24) Zhou, Z.; Zhao, J. J.; Chen, Z. F.; Gao, X. P.; Lu, J. P.; Schleyer, P. v. R.; Yang, C. K. *J. Phys. Chem. B* **2006**, *110*, 2529.

(25) Kresse, G.; Hafner, J. *J. Phys.: Condens. Matter.* **1994**, 6.

(26) Kresse, G.; Hafner, J. *Phys. Rev. B: Condens. Matter Mater. Phys.* **1994**, *49*, 14251.

(27) Ceperley, D. M.; Alder, B. J. *Phys. Rev. Lett.* **1980**, *45*, 566.

(28) Vanderbilt, D. *Phys. Rev. B: Condens. Matter Mater. Phys.* **1990**, *41*, 7892.

(29) Christensen, N. E.; Gorczyca, I. *Phys. Rev. B: Condens. Matter Mater. Phys.* **1994**, *50*, 4397.

(30) Zhou, Z.; Zhao, J. J.; Chen, Y. S.; Schleyer, P. v. R.; Chen, Z. F. *Nanotechnology* **2007**, *18*, 424023.

(31) Zhao, M. W.; Xia, Y. Y.; Liu, X. D.; Tan, Z. Y.; Huang, B. D.; Song, C.; Mei, L. M. *J. Phys. Chem. B* **2006**, *110*, 8764.